Magnetization Dynamics in a Current-Driven Magnetic Nano-Pillar with Dipole-Dipole Coupling between Magnetic Layers

Oleksandr Dmytriiev[1,3], Thomas Meitzler[2], Elena Bankowski[2], Vasil Tiberkevich[1], and Andrei Slavin[1]
[1] *Department of Physics, Oakland University, Rochester, Michigan 48309, USA*
[2] *U.S. Army TARDEC, Warren, Michigan 48397, USA*
[3] *Institute of Magnetism, Vernadski Blvd. 36, Kyiv-142, Ukraine*
(Dated: September 25, 2009)

The small-amplitude uniform magnetization excitations in a magnetic nano-pillar with two ferromagnetic layers coupled by the dipole-dipole interaction are considered. We showed that the dipole magnetic field in this system can be fully described by two diagonal tensors for every layer The spectrum of coupled oscillations is found. It consists of two modes, the lower mode is quasi-antisymmetric at small bias fields and excited by current, the upper mode is quasi-symmetric at small bias fields and excited by microwave magnetic field. It is demonstrated that this spectrum can be described by the traditional Kittel expressions with decreased saturated magnetization and renormalized external magnetic field. We also demonstrated that for realistic nano-pillar parameters this renormalization does not exceed 10 % for the lower quasi-antisymmetric mode at small bias fields, and 50 % for the upper quasi-symmetric mode at small bias fields.

PACS numbers:

I. INTRODUCTION

The physics of magnetic multi-layer systems with layers of ferromagnetic materials separated by non-magnetic spacers with thickness in the nano-metric range is very rich and these systems have a lot of practical applications. It is well known that the dipole-dipole interaction in such kind of systems plays crucial role due to that the ferromagnetic layers are placed close to each other comparing to their lateral sizes and it leads to substantial spectrum modification comparing to single layer. Multi-layer thing films have been existed and studied for more than thirty years while active study of spin dynamics in multi-layer patterned magnetic structures started relatively recently about a decade ago when advances in lithography made possible the realization of patterns of nano-metric magnetic elements with controlled shape and dimensions.

Such kind of systems, in which the influence of dipole magnetic interaction on the spectrum have investigated recently, are ordered arrays of long magnetic stripes with micro-metric width[6,7] and an array of long magnetic stripes which are situated over a continuous magnetic film[5].

Another class of patterned system where dipole interaction plays important role are nano-scale spin-torque oscillators (STO). Since the first observations of microwave generations by STO[11] extensive experimental results have been reported concerning the frequency measurements of this generation in low-amplitude regime for the large variety of magnetic multi-layer nano-systems. In these experiments, the dependence of the measured frequency on an bias magnetic field is described well by the Kittel expression for both in-plane and perpendicularly magnetized multi-layers provided the magnetization of the free layer is essentially decreased by 30 to 75 percent depending on a system[4,11,12,15,18]. The prevalent explanation of this fact is the necessity of taking into account of a dipole-dipole interaction between layers.

Micro-structured and nano-structured ferromagnets can also be used efficiently as microwave absorbers in monolithic microwave integrated circuit due to the fact that their FMR frequency can be widely tuned in the range of several tens of gigahertz by applying external magnetic fields. However constant application of external magnetic fields is inconvenient from point of view of low electric power consuming. In order to resolve this problem it was proposed to control the FMR frequency by using dipole magnetic field in patterned magnetic multilayers[16,17].

In the present paper, we theoretically studied influence of dipole-dipole interaction on the spatially-uniform spin wave modes in in-plane magnetized two-layered magnetic nano-pillar shown on Fig. 1. For simplicity, we did not take into account in-plane anisotropy (i.e., we assumed that the magnetic layers are patterned intro circular disks) and assumed that in each disk the excited mode has spatially-uniform profile. The later assumption is justified for small nano-scale disks, in which strong exchange interaction prohibits excitation of higher spatial modes.

II. THE SYSTEM OF EQUATIONS

The dynamics of coupled magnetization oscillations exited by a spin polarized current in a two layer nano-pillar is described by two Landau-Lifshits-Gilbert-Slonczewski (LLGS) equations[2,3,19–21]:

$$\frac{\partial \mathbf{M}_j}{\partial t} = \gamma \left[\mathbf{H}_{eff,j} \times \mathbf{M}_j\right] + \mathbf{T}_{D,j} + \mathbf{T}_{S,j} + \mathbf{T}_{F,j}(t), \quad (1)$$

where $j = 1, 2$ and $\mathbf{M}_j$ is the magnetization of the j-th layer. The first term on the right-hand side of Eqs. (1) describes conservative precession of the magnetization

Report Documentation Page

Form Approved
OMB No. 0704-0188

1. REPORT DATE	2. REPORT TYPE	3. DATES COVERED
25 SEP 2009	**N/A**	**-**

4. TITLE AND SUBTITLE	5a. CONTRACT NUMBER
Magnetization Dynamics in a Current-Driven Magnetic Nano-Pillar with Dipole-Dipole Coupling between Magnetic Layers (PREPRINT)	5b. GRANT NUMBER
	5c. PROGRAM ELEMENT NUMBER
6. AUTHOR(S)	5d. PROJECT NUMBER
Oleksandr Dmytriiev; Thomas Meitzler; Elena Bankowski; Vasil Tiberkevich; Andrei Slavin	5e. TASK NUMBER
	5f. WORK UNIT NUMBER
7. PERFORMING ORGANIZATION NAME(S) AND ADDRESS(ES)	8. PERFORMING ORGANIZATION REPORT NUMBER
US Army RDECOM-TARDEC 6501 E 11 Mile Rd Warren, MI 48397-5000, USA Department of Physics, Oakland University, Rochester, Michigan, USA Institute of Magnetism, Vernadski Blvd. 36, Kyiv-142, Ukraine	**20255**
9. SPONSORING/MONITORING AGENCY NAME(S) AND ADDRESS(ES)	10. SPONSOR/MONITOR'S ACRONYM(S)
US Army RDECOM-TARDEC 6501 E 11 Mile Rd Warren, MI 48397-5000, USA	**TACOM/TARDEC/RDECOM**
	11. SPONSOR/MONITOR'S REPORT NUMBER(S) **20255**

12. DISTRIBUTION/AVAILABILITY STATEMENT
Approved for public release, distribution unlimited

13. SUPPLEMENTARY NOTES
Submitted for publication in Journal of Applied Physics, The original document contains color images.

14. ABSTRACT

15. SUBJECT TERMS

16. SECURITY CLASSIFICATION OF:			17. LIMITATION OF ABSTRACT	18. NUMBER OF PAGES	19a. NAME OF RESPONSIBLE PERSON
a. REPORT	b. ABSTRACT	c. THIS PAGE			
unclassified	**unclassified**	**unclassified**	**SAR**	**9**	

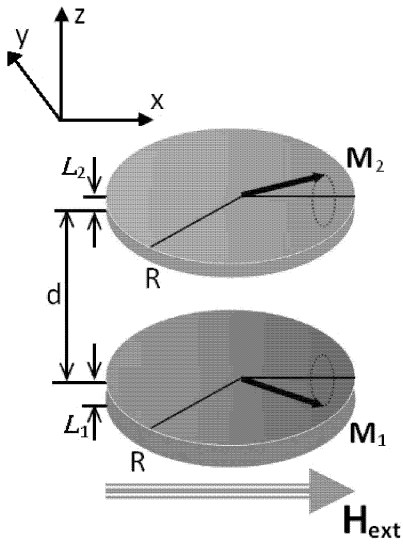

FIG. 1: (color online) Nano-pillar with two ferromagnetic layers coupled by the dipole-dipole interaction in constant bias magnetic field $\mathbf{H}_{ext}$, directed along x-axes. Thicknesses of the layers $L_{1,2}$ and the distance d between them are much smaller than the layer radius R. The layers have the same saturation magnetization $M_1 = M_2 = M$ ($4\pi M = 8kOe$, which is typical for permalloy).

vector $\mathbf{M}_j$ about the direction of the effective magnetic field $\mathbf{H}_{eff,j}$, where $\gamma \approx 2\pi \cdot 2.8 GHz/kOe$ is the modulus of the gyromagnetic ratio. The structure of $\mathbf{H}_{eff,j}$ will be clarified bellow. The second term

$$\mathbf{T}_{D,j} = \frac{\alpha\gamma}{M}\left[\mathbf{M}_j \times [\mathbf{H}_{eff,j} \times \mathbf{M}_j]\right]$$

is dissipative torque that describes the energy dissipation, where α is the damping constant. The third term

$$\mathbf{T}_{S,j} = \mp\frac{\sigma_j I}{M^2}\left[\mathbf{M}_j \times [\mathbf{M}_j \times \mathbf{M}_{j'}]\right]$$

is the Slonczewski-Berger spin-transfer torque that describes interaction of the magnetization $\mathbf{M}_j$ with a spin-polarized current passing through the layers, it depends on orientation of the magnetization of the j'-layer , where $j' = 3 - j$ and I is a current, $\sigma_j = g\varepsilon\mu_B/2eML_j$ (g is the spectroscopic Lande factor, ε_j is a dimensionless spin-polarization efficiency, μ_B is the Borh magneton, e is the modulus of an electron charge, L_j is the thickness of the j-th layer). We will choose positive direction of a current the way that the sign "$-$" is taken for the first layer and "$+$" for the second one. This means that damping caused by a spin-polarized current will be positive for the first layer and negative for the second one. If we neglect the magnetization dynamic in the first layer and assume that its magnetization is fixed it will correspond the well studied case of magnetization excitation only in one (second) layer which is called "free" in this case (the first layer is called "fixed"). The last term

$$\mathbf{T}_{F,j} = \gamma\left[\mathbf{h}_\sim(t) \times \mathbf{M}_j\right]$$

is a time-dependent torque which describes action of a microwave magnetic field, where $\mathbf{h}_\sim(t) = \mathbf{h}_\sim \cos(\omega_{ext}t)$ is a microwave magnetic field, $\mathbf{h}_\sim$ is its amplitude and ω_{ext} is its frequency. We will assume that the vector $\mathbf{h}_\sim$ is perpendicular to static bias magnetic field $\mathbf{H}_{ext}$.

Typically, the first, conservative magnetization precession term in the LLGS equation is much larger than all the other terms: dissipation, spin-transfer torque, and action of a microwave magnetic field and we can use the following spin-wave formalism[8,21]. The solution of the considered problem is divided into two steps. At the first step, we consider the influence of conservative precessional torque and obtain spin wave modes by solving the conservative Landau-Lifshits equation with precessional term only. At the second step, we analyze the influence of damping and excitation torques on the dynamics of previously found spin wave modes. It is usually possible to treat damping and excitation as small perturbations, which allows one to obtain simple and understandable analytical results.

The coupled magnetization dynamic which we will consider can be excited by either current or microwave magnetic field.

III. THE DIPOLAR MAGNETIC FIELD PARAMETERS FOR TWO LAYER NANO-PILLAR

The Landau-Lifshits equation that describes non decaying excitations in two layer nano-pillar looks as follows:

$$\frac{\partial \mathbf{M}_j}{\partial t} = \gamma\left[\mathbf{H}_{eff,j} \times \mathbf{M}_j\right], \qquad j = 1, 2. \tag{2}$$

The effective magnetic field $\mathbf{H}_{eff,j}$ for j-th layer, which enters the LLGS equation, consists of the external bias magnetic field $\mathbf{H}_{ext}$ and magnetodipolar fields, created by each of the two layers:

$$\mathbf{H}_{eff,j} = \mathbf{H}_{ext} + \sum_{k=1}^{2} \mathbf{H}_{j,k}.$$

Here $\mathbf{H}_{j,k}$ dipolar field, created by the k-th layer and acting on the j-th one. The dipolar magnetic field created by a layer depends on a spatial variable (it is spatially uniform only inside an uniform magnetized ellipse[14]). We consider spatially-uniform spin wave excitations so the field $\mathbf{H}_{j,k}$ should be understood as the real spatially-nonuniform field $\mathbf{H}_k(\mathbf{r})$, which is created by the k-th layer, averaged over the volume V_j of the j-th one:

$$\mathbf{H}_{j,k} = \frac{1}{V_j}\int\limits_{V_j} \mathbf{H}_k(\mathbf{r}_j)d\mathbf{r}_j$$

For uniformly magnetized k-th layer the dipolar field $\mathbf{H}_k(\mathbf{r})$ can be written as follows:

$$\mathbf{H}_k(\mathbf{r}) = -4\pi\widehat{N}_k(\mathbf{r})\mathbf{M}_k, \tag{3}$$

where the position-dependent demagnetization tensor $\widehat{N}_k(\mathbf{r})$ is given by the expression[1] :

$$\left(\widehat{N}_k(\mathbf{r})\right)_{sp} = -\frac{1}{4\pi}\cdot\frac{\partial^2}{\partial x_s \partial x_p}\int\limits_{V_k}\frac{d\mathbf{r}_k}{|\mathbf{r}-\mathbf{r}_k|}. \tag{3a}$$

This expression for the dipolar field $H_k(\mathbf{r})$ is valid both inside and outside of the k-th layer. If we calculate derivatives before taking the integral we will get nothing else but the ordinary expression for magnetic field produced by a point dipole. But in this case, the integral will logarithmically diverge for the diagonal matrix elements when the spatial variable $\mathbf{r}$ takes a value inside the k-th layer. The trace of the tensor $\widehat{N}_k(\mathbf{r})$ equals

$$\mathtt{Tr}\widehat{N}_k(\mathbf{r}) = -\frac{1}{4\pi}\int\limits_{V_k}\mathbf{\Delta}_{\mathbf{r}}\frac{d\mathbf{r}_k}{|\mathbf{r}-\mathbf{r}_k|} = \int\limits_{V_k}\delta(\mathbf{r}-\mathbf{r}_k)d\mathbf{r}_k, \tag{3b}$$

where $\delta(\mathbf{r}-\mathbf{r}_k)$ is the Dirac delta-function.

By using the above formulas, we can write the dipolar fields $\mathbf{H}_{j,k}$ as

$$\mathbf{H}_{j,k} = -4\pi\widehat{N}_{jk}\mathbf{M}_k,$$

where

$$\widehat{N}_{jk} = \frac{1}{V_j}\int\limits_{V_j}\widehat{N}_k(\mathbf{r}_j)d\mathbf{r}_j \tag{3c}$$

are effective dimensionless self- (for $j=k$) and cross- (for $j\neq k$) demagnetization tensors, which fully characterize the dipole-dipole interaction in our system. The self-demagnetization tensor is also called the tensor of demagnetizing coefficients.

It should be noted that the spatially-nonuniform self-demagnetization tensor $\widehat{N}_j(\mathbf{r}_j)$ for a cylinder (and correspondingly for a disk) were calculated in paper[10] but we need spatially-uniform (averaged over a volume) both self- and cross- demagnetization tensors.

Thus, the effective field for the j-th layer $\mathbf{H}_{eff,j}$ takes a simple form:

$$\mathbf{H}_{eff,j} = \mathbf{H}_{ext} - 4\pi\sum_{k=1}^{2}\widehat{N}_{jk}\mathbf{M}_k. \tag{4}$$

The demagnetization tensors $\widehat{N}_{jk}$ are symmetrical, their traces are

$$\mathtt{Tr}\left(\widehat{N}_{jk}\right) = \delta_{jk}$$

where δ_{jk} is the Kronecker symbol, and and different cross-demagnetization tensors are connected by the expression:

$$V_j\widehat{N}_{jk} = V_k\widehat{N}_{kj}, \qquad j\neq k.$$

These properties directly follow from Eqs. (3a), (3b), (3c) and they are valid in a general case, i.e. for a system of magnetic bodies of arbitrary shapes.

Due to in-plane symmetry of the considered system of two disks, demagnetization tensors $\widehat{N}_{jk}$ are diagonal in the coordinate system represented on Fig. 1 and can be represented as follows:

$$\widehat{N}_{jk} = \begin{pmatrix} \rho_{jk} & 0 & 0 \\ 0 & \rho_{jk} & 0 \\ 0 & 0 & \delta_{jk}-2\rho_{jk} \end{pmatrix} \tag{5}$$

i.e. each tensor depends only on one parameter ρ_{jk}. In the limit of very thin disks $\rho_{jk}\to 0$, and dipolar coupling between layers vanishes. By using Eqs. (3a) and (3c), the dipolar magnetic field parameters ρ_{jk} can be expressed in terms of six-fold multiple integral as follows:

$$\rho_{jk} = \frac{1}{8\pi V_j}\int\limits_{V_j}d\mathbf{r}_j\int\limits_{V_k}d\mathbf{r}_k\left(\frac{3(z_j-z_k)^2-|\mathbf{r}_j-\mathbf{r}_k|^2}{|\mathbf{r}_j-\mathbf{r}_k|^5}\right). \tag{6}$$

This integral can be taken over an area of the first and the second layers after introducing new variables of integration, one of which is the difference of in-plane radius-vectors of the first and the second layers and the other one is in-plane radius-vector of one of the layers. The integral (6) can be simplified to

$$\rho_{jk} = \frac{1}{2\pi}\cdot\frac{L_k}{R}\int\limits_0^1 dz_j\int\limits_0^1 dz_k f\left(\frac{L_j}{R}z_j+\frac{L_k}{R}z_k+\frac{d}{R}\right), \tag{6a}$$

for $j\neq k$ and

$$\rho_{jj} = \frac{1}{2\pi}\cdot\frac{L_j}{R}\int\limits_0^1 dz(1-z)f\left(\frac{L_j}{R}z\right), \tag{6b}$$

for $j=k$. Here

$$f(\alpha) = \left[\frac{2+\alpha^2}{\alpha}K\left(-\frac{4}{\alpha^2}\right)-\alpha E\left(-\frac{4}{\alpha^2}\right)\right],$$

where $K(\xi)$ and $E(\xi)$ are complete elliptic integrals of the first and second kind.

The function $f(\alpha)$ has a logarithmic singularity when $\alpha\to 0$. Extracting this singularity and leaving terms up to $O(\alpha^2\ln(\alpha))$ we have the approximate analytic expressions for the dipolar magnetic field parameters in a case of thin disks ($L_{1,2}\ll R$ and $d\ll R$):

$$\begin{aligned}\rho_{jk} = {} & \frac{1}{2\pi}\frac{L_k}{R}\cdot C- \\ & -\frac{1}{4\pi(L_j/R)}\left[F\left(\frac{d}{R}\right)-F\left(\frac{d+L_j}{R}\right)-\right. \\ & \left.-F\left(\frac{d+L_k}{R}\right)+F\left(\frac{d+L_j+L_k}{R}\right)\right],\end{aligned} \tag{6c}$$

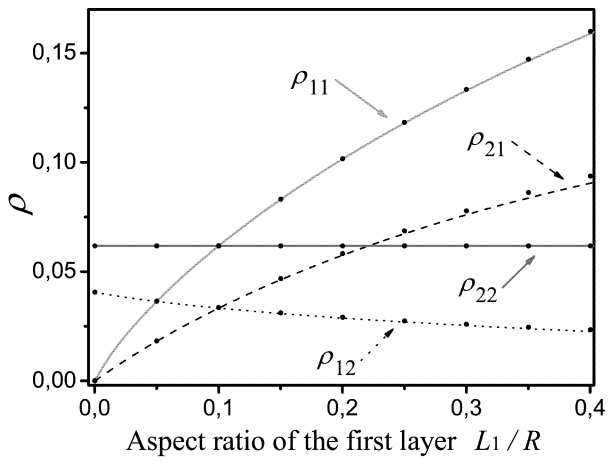

FIG. 2: (color online) The dimensionless dipolar magnetic field parameters ρ_{jk}, which define self- and cross-demagnetization tensors for the system of two thin disks, as functions of the aspect ratio of the first layer L_1/R. Aspect ratio of the second layer and distance between layers are fixed: $L_2/R = 1/10, d/R = 1/25$. **Solid, dashed and dotted lines**: Approximate analytical expressions (6c) and (6d). **Dots**: Exact expressions (6a) and (6b).

for $j \neq k$ and

$$\rho_{jj} = \frac{1}{2\pi}\frac{L_j}{R}\cdot\left[C - \ln\left(\frac{L_j}{R}\right)\right], \tag{6d}$$

for $j = k$. Here $C = -1/2 + \ln(8)$ and $F(\zeta) = \zeta^2 \ln|\zeta|$. It should be noted that Eq. (6d) can be obtained from Eq. (6c) by substituting $L_k = L_j$ and $d = -L_j$.

One can see from expressions (6a) and (6b) the cross-demagnetization tensors depend on aspect ratio of both layers and relative distance between them: $\widehat{N}_{jk} = \widehat{N}_{jk}(L_j/R, L_k/R, d/R)$, the self-demagnetization tensors depend on aspect ratio of correspondent layer: $\widehat{N}_{jj} = \widehat{N}_{jj}(L_j/R)$. When $L_j/R \to 0$ we have that $\rho_{jj} \to 0$ and $\rho_{j'j} \to 0$ ($j' = 3 - j$). In this case the self-demagnetization tensor of the j-th layer N_{jj} passes into the tensor of demagnetizing coefficients of unbounded ferromagnetic film and the cross-demagnetization tensor $N_{j'j}$, which describes the action of the dipolar magnetic field created by the j-th layer on the j'-th one, passes into zero tensor.

On Fig 2, the dimensionless dipolar magnetic field parameters ρ_{jk} are represented as a function of the aspect ratio of the first layer L_1/R. Aspect ratio of the second layer and distance between layers are fixed: $L_2/R = 1/10, d/R = 1/25$.

IV. THE SPECTRUM OF COUPLED LINEAR EXCITATIONS

We consider a case of tangentially magnetized nano-pillar and large enough constant bias magnetic field, when the ground state of the system is the parallel orientations of magnetization in both layers. We will return later to the question on the magnitude of constant bias magnetic field when the parallel orientations of magnetization is stable. We linearize Eq. (2) by the substitution:

$$\mathbf{M}_j(t) = M\left[\mathbf{x} + (\mathbf{m}_j e^{i\omega t} + c.c.)\right]. \tag{7}$$

The first term here is the equilibrium orientation of the magnetization vectors, whereas the second term describes small-amplitude (linear) spin wave modes. The vectors $\mathbf{m}_j$ are orthogonal to the unit vector $\mathbf{x}$ in linear approximation. Keeping only the linear in $\mathbf{m}_j$ terms yields the following eigenvalue problem for determination of frequencies ω and profiles $\mathbf{m}_j$ of spin waves:

$$i\omega\mathbf{m}_j = \gamma\mathbf{x}\times\left[(H_{ext} - 4\pi\sum_{k=1}^{2}\rho_{jk}M)\mathbf{m}_j + 4\pi M\sum_{k=1}^{2}\widehat{N}_{jk}\mathbf{m}_k\right] \tag{8}$$

Condition of solvability of this system determines frequencies of spin wave modes:

$$\left(\omega^2 - \widetilde{\omega}_1^2\right)\left(\omega^2 - \widetilde{\omega}_2^2\right) = \Phi_{int}, \tag{9}$$

where

$$\Phi_{int} = -4\rho_{12}\rho_{21}\omega_M^2\left(\omega^2 + \rho_{12}\rho_{21}\omega_M^2 - \omega_{h,1}\omega_{h,2} - \frac{\widetilde{\omega}_1^2\widetilde{\omega}_2^2}{4\omega_{h,1}\omega_{h,2}}\right), \tag{9a}$$

Here $\omega_M = 4\pi\gamma M$, $\omega_{h,j} = \gamma h_j$. The field h_j is the static magnetic field acting on the j-th layer, i.e. it is external field + static dipolar field created by the other layer:

$$h_j = H_{ext} - 4\pi\rho_{jj'}M,$$

where $j' = 3 - j$. The static dipolar magnetic field $-4\pi\rho_{jj'}M$ created inside the j-th layer by the j'-th one can reach a half a kOe for realistic nano-pillar parameters (it can be seen from Fig 2). Frequency $\widetilde{\omega}_j$ is the precession frequency of the j-th layer with taking into account of only static coupling to the other layer:

$$\widetilde{\omega}_j = \gamma\sqrt{h_j(h_j + 4\pi[1 - 3\rho_{jj}]M)}.$$

The term Φ_{int} describes dynamic coupling between two layers and depends on the frequency ω. When $L_j/R \to 0$, what means either the thickness of the j-th layer tends to zero or its radius tends to infinity, the dipolar magnetic field produced by the j-th layer vanishes outside of it. This lead to vanishing of dynamic coupling between

layers and function Φ_{int} tends to zero. The dynamic coupling between layers is maximum when the layers have the same thickness. The term Φ_{int} was neglected in all previous studies.

The solutions of Eq. (9) can be approximately described by the traditional Kittel expression with renormalized external field and saturation magnetization:

$$\omega_{1,2} = \gamma\sqrt{\left(H_{ext} - \widetilde{H}_{1,2}\right)\left(H_{ext} - \widetilde{H}_{1,2} + 4\pi\widetilde{M}_{1,2}\right)}, \tag{10}$$

where

$$\widetilde{H}_1 = 0, \qquad \widetilde{H}_2 = 4\pi(\rho_{12} + \rho_{21})M$$

and

$$\widetilde{M}_1 = \left(1 - 3\frac{\rho_{11}\rho_{21} + \rho_{22}\rho_{12} + 2\rho_{12}\rho_{21}}{\rho_{12} + \rho_{21}}\right)M,$$
$$\widetilde{M}_2 = \left(1 - 3\frac{\rho_{11}\rho_{12} + \rho_{22}\rho_{21} - 2\rho_{12}\rho_{21}}{\rho_{12} + \rho_{21}}\right)M.$$

The frequencies (10) are exact solutions of Eq. (9) in two limit cases: (i) when the layers have the same thickness and (ii) when the thickness of one of the layers tends to zero.

The parameters $\widetilde{H}_j$ are found by determining zeros of the solutions of Eq. (9). The expressions for renormalized magnetization $\widetilde{M}_{1,2}$ are the simplest ones that give correct result in both limit cases mentioned above.

For symmetrical system (both layers have identical thicknesses), mode with the frequency ω_1 corresponds to symmetric excitations (the magnetization precession in both layers have the same phases), whereas mode with the frequency ω_2 describes antisymmetric excitations (opposite phases of precession in both layers). For different thicknesses of the layers one can still classify the mode ω_1 as quasi-symmetric, and mode ω_2 as quasi-antisymmetric.

The frequencies of coupled linear excitations are represented on Fig. 3. One can see that expressions (10) fit the solution of secular Eq. (9) with high accuracy at small bias magnetic fields. When

$$H_{ext} = \widetilde{H}_2(4\pi\widetilde{M}_2 - \widetilde{H}_2)/(4\pi(\widetilde{M}_1 - \widetilde{M}_2) - 2\widetilde{H}_2)$$

the curves that correspond to approximate expressions (10) intersect while the curves that correspond to the solution of secular Eq. (9) do not. The modes described by secular Eq. (9) change their symmetry near this point, while the modes described by approximate expressions (10) retain their symmetry. On Fig 4, the maximum and minimum angle between the vectors $\mathbf{m}_1$ and $\mathbf{m}_2$, which describe the coupled linear spin wave excitation in the first and the second layer respectively, for frequencies that are the solutions of Eq. (9) are represented. While calculating we put: $L_1/R = 1/5, L_2/R = 1/10, d/R = 1/25$.

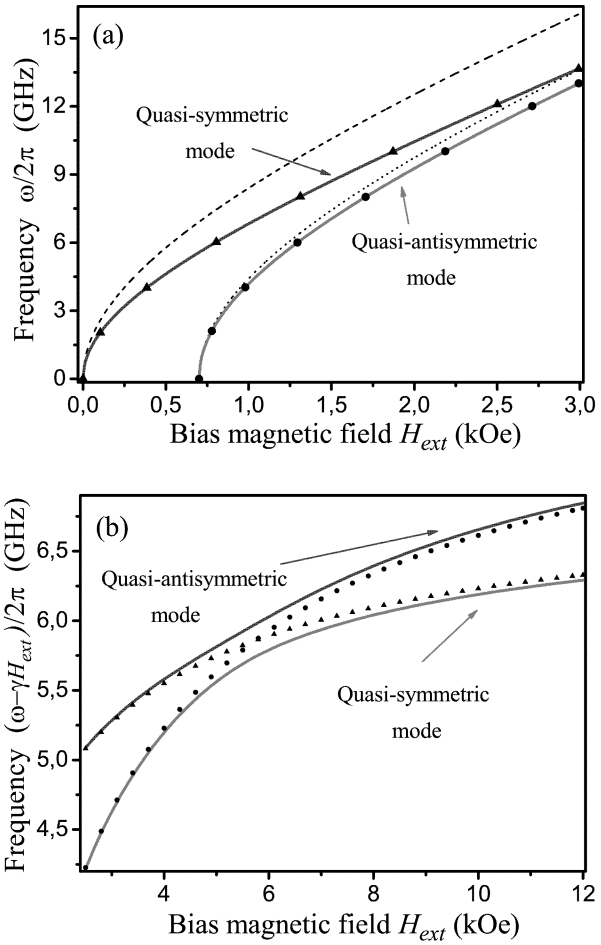

FIG. 3: (color online) **(a)** The frequencies of linear coupled excitations in a two layer nano-pillar as a function of bias magnetic field. **Solid lines**: The exact solutions of secular Eq. (9). **Triangles and dots**: The frequencies $\omega_1/2\pi$ and $\omega_2/2\pi$ respectively (approximate expressions (10)). **Dashed and dotted lines**: The traditional Kittel expressions for in-plane magnetized ferromagnetic film[13]: $\omega_{K,1} = \gamma\sqrt{H_{ext}(H_{ext} + 4\pi M)}$ and $\omega_{K,2} = \gamma\sqrt{(H_{ext} - \widetilde{H}_2)(H_{ext} - \widetilde{H}_2 + 4\pi M)}$ respectively. **(b)** The frequencies $(\omega - \gamma H_{ext})/2\pi$ as a function of bias magnetic field. **Solid lines**: The exact solutions of secular Eq. (9). **Triangles and dots**: $(\omega_1 - \gamma H_{ext})/2\pi$, $(\omega_2 - \gamma H_{ext})/2\pi$ respectively (approximate expressions (10)). While calculating we put: $L_1/R = 1/5, L_2/R = 1/10, d/R = 1/25$.

The parallel magnetization ground state is stable when external bias magnetic field is larger than $\widetilde{H}_2$ ($\widetilde{H}_2 = 0.7kOe$ for the spectrum represented on Fig. 3) otherwise one of the frequencies is complex what leads to instability of the ground state.

As one can see from Fig. 3 the both modes lie lower corresponding Kittel modes, that means the both mode correspond to effective decrease of magnetization and the decrease for quasi-symmetric mode is larger. The rela-

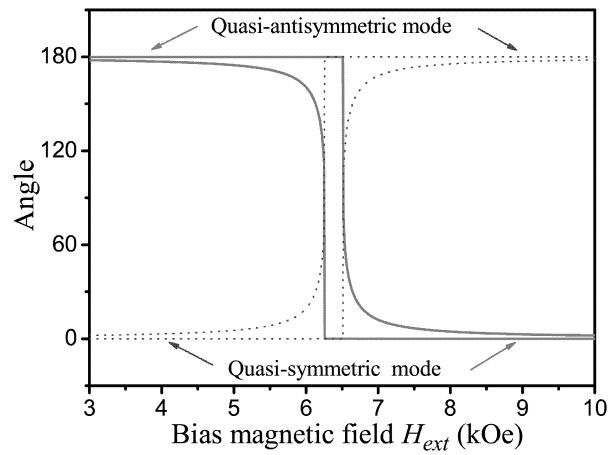

FIG. 4: (color online) The maximum and minimum angle between the vectors $\mathbf{m}_1$ and $\mathbf{m}_2$, which describe the coupled linear spin wave excitation in the first and the second layer respectively, for frequencies that are the solutions of Eq. (9) as a function of a bias magnetic field. **Solid red lines**: for lower mode on Fig 3. **Dashed blue lines**: for upper mode on Fig 3. While calculating we put: $L_1/R = 1/5, L_2/R = 1/10, d/R = 1/25$.

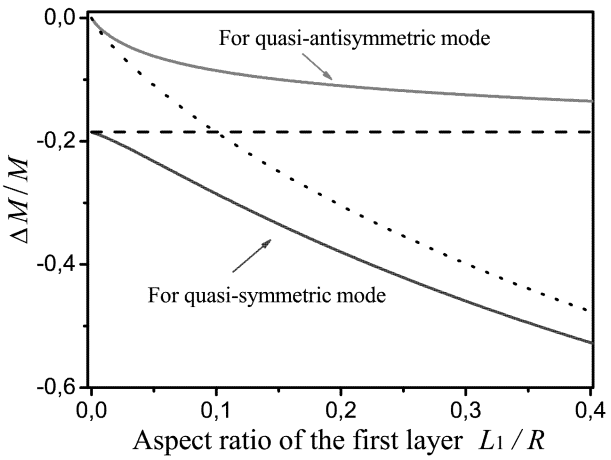

FIG. 5: (color online) **Solid lines**: Relative decrease of effective magnetization $(\widetilde{M}_{1,2} - M)/M$ for both quasi-symmetric and quasi-antisymmetric modes with respect to the magnetization of unbounded ferromagnetic film. **Dotted and dashed lines**: The effective decrease of magnetization for the first and the second isolated (uncoupled) layers, respectively. While calculating we fixed the thickness of the second layer and the distance between layers: $L_2/R = 1/10, d/R = 1/25$.

tive decrease of magnetization $(\widetilde{M}_{1,2} - M)/M$ with respect to the magnetization of unbounded ferromagnetic film as a function of aspect ratio of the first layer is represented on Fig. 5. While calculating we fixed the thickness of the second layer and the distance between layers: $L_2/R = 1/10, d/R = 1/25$. One can see from Fig. 5 when the difference in layer thickness increases (it means the coupling between layers get weaker) the effective decrease of magnetization occurs mainly due to corresponding self-demagnetization tensors (the tensors of demagnetizing coefficients). As one can see from Fig. 5 the effective decrease of magnetization for upper quasi-symmetric mode at small bias fields can reach 50 % for still realistic nano-pillar parameters (due to self-demagnetization tensor mainly) and effective decrease of magnetization for lower quasi-antisymmetric mode can only be about 10%.

V. THE EXCITATION OF COUPLED LINEAR SPIN WAVE MODES BY CURRENT AND MICROWAVE MAGNETIC FIELD

The eigenvalue problem (8) give us four different frequencies (two positive and two negative). It means all eigenvectors $\{\mathbf{m}_1^{(\nu)}, \mathbf{m}_2^{(\nu)}\}$ (index $\nu = 1, 4$ numerate different eigenvalues), which describe the coupled linear spin wave excitation in the first and second layers, are linear independent and they form the linear space $\mathbb{C}^2 \times \mathbb{C}^2$. They are orthogonal with respect to the inner product[9]:

$$-i \sum_{j=1}^{2} V_j \mathbf{x} \cdot [\mathbf{m}_j^{(\nu)*} \times \mathbf{m}_j^{(\nu')}] = N_\nu \delta_{\nu\nu'},$$

where N_ν is a norm (defined by this expression) and $\delta_{\nu\nu'}$ is the Kronecker symbol.

We can expand the solution of linearized Eq. (1) in a full set of functions defined by eigenvalue problem (8). After substitution

$$\mathbf{M}_j(t) = M \left[\mathbf{x} + \sum_{\nu=1}^{4} (\mathbf{m}_j^{(\nu)} c_\nu(t) + c.c.) \right] \qquad (11)$$

into Eq. (1) linearizing it and taking the inner product with $\{\mathbf{m}_1^{(\nu)}, \mathbf{m}_2^{(\nu)}\}$ we get the system of equations that is equivalent to linearized Eq. (1):

$$\frac{dc_\nu(t)}{dt} = \sum_{\nu'=1}^{4} (\omega_\nu \delta_{\nu\nu'} + i[\alpha Q_{\nu\nu'} - I P_{\nu\nu'}]) c_{\nu'} + \\ + S_\nu \cos(\omega_{ext} t), \qquad (12)$$

where ω_ν is a frequency of linear coupled excitation defined by a secular Eq. (9) and

$$Q_{\nu\nu'} = -\frac{\omega_{\nu'}}{N_\nu} \sum_{j=1}^{2} V_j (\mathbf{m}_j^{(\nu)*} \cdot \mathbf{m}_j^{(\nu')}) \qquad (12a)$$

are matrix elements which define damping caused by the damping torque,

$$P_{\nu\nu'} = -\frac{i}{N_\nu} \sum_{j=1}^{2} \sigma_j V_j \, \mathbf{x} \cdot [\mathbf{m}_j^{(\nu)*} \times (\mathbf{m}_2^{(\nu')} - \mathbf{m}_1^{(\nu')})] \qquad (12b)$$

are matrix elements which define negative damping caused by the Slonczwski-Berger torque. Both matrixes $\hat{Q}$ and $\hat{P}$ are real. And

$$S_\nu = \frac{i\gamma}{N_\nu}\sum_{j=1}^{2} V_j(\mathbf{m}_j^{(\nu)*}\cdot\mathbf{h}_\sim), \qquad (12c)$$

we assumed that the vector of amplitude of microwave magnetic field $\mathbf{h}_\sim$ is perpendicular to constant bias magnetic field $\mathbf{H}_{ext}$.

We will use the fact that conservative magnetization precession term in the LLGS equation is much larger than dissipation, spin-transfer torques, and action of a microwave magnetic field and we will treat them as small perturbation so we will solve Eq. (12) using perturbation theory.

We will consider the action of current and microwave magnetic field separately. We will consider the excitation of coupled linear spin wave modes by current first so we consider Eq. (12) with $S_\nu = 0$. We will use the following substitution $c_\nu = e^{i\Omega_\nu t}$. We have

$$\sum_{\nu'=1}^{4}([\Omega_\nu - \omega_\nu]\delta_{\nu\nu'} - i[\alpha Q_{\nu\nu'} - IP_{\nu\nu'}])c_{\nu'} = 0, \qquad (13)$$

here Ω_ν is a complex frequency, the real part of which is the frequency of coupled linear excitation and imaginary part is the damping. The imaginary part depends on a current I and the Gilbert constant α. By equating it to zero we get the threshold current I_{th} for excitation of coupled linear spin wave modes.

The first order of the perturbation theory give us:

$$\Omega_\nu = \omega_\nu + i[\alpha Q_{\nu\nu} - IP_{\nu\nu}]. \qquad (14)$$

One can see the damping is linear with respect to current I and the Gilbert constant α in the first order of the perturbation theory. The second order of the perturbation theory is real and give us the adjustment to the frequency of the coupled linear excitation.

The threshold current for excitation of coupled linear spin wave modes as a function of a bias magnetic field is represented on Fig. 6. One can see that current excites lower (quasi-antisymmetric) mode at small bias fields and upper mode (which passes from quasi-symmetric to quasi-antisymmetric with bias field increase) at large bias fields. It should be noted that both frequencies (see Fig. 3) are close to each other, do not intersect at large bias fields and so it is not very important practically which mode is excited at these bias fields.

By using expression (14), the expression for threshold current at small bias fields can be written as follows:

$$I_{th} = \alpha\frac{Q_{22}}{P_{22}}, \qquad (15)$$

where Q_{22} and P_{22} are the matrix elements (12a) and (12b) calculated on the eigenfunctions which correspond to lower mode, which is quasi-antisymmetric at small bias fields.

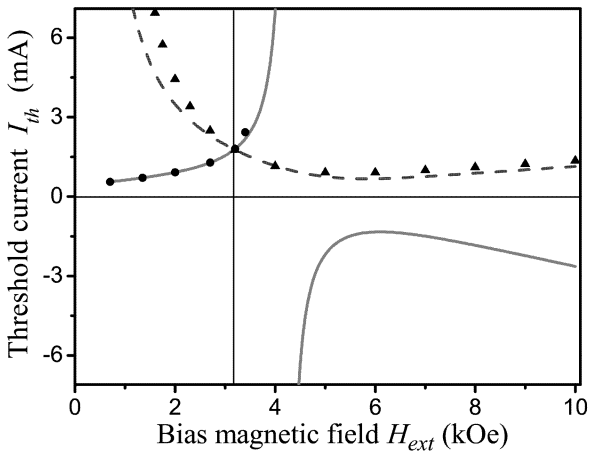

FIG. 6: (color online) The threshold current for excitation of coupled linear spin wave modes represented on Fig. 3 as a function of a bias magnetic field. While calculating we put: $L_1/R = 1/5, L_2/R = 1/10, d/R = 1/25, R = 50nm, \alpha = 0.01, \varepsilon_1 = \varepsilon_2 = 1$. **Solid and dashed lines**: The threshold current for excitation of lower mode (quasi-antisymmetric one at small bias external fields) and upper mode (quasi-symmetric one at small bias external fields), respectively, obtained from approximate Eq. (14). **Dots and triangles**: The same threshold current obtained from Eq. (13).

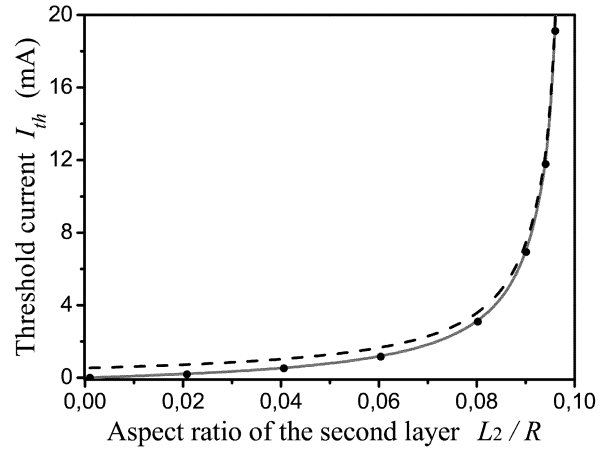

FIG. 7: (color online) The threshold current for excitation of lower mode, which is quasi-antisymmetric one at small bias fields, as a function of aspect ratio of the second layer L_2/R when external bias magnetic field $H_{ext} = 3kOe$. While calculating we put: $L_1/R = 1/10, d/R = 1/25, R = 50nm, \alpha = 0.01, \varepsilon_1 = \varepsilon_2 = 1$. **Solid line**: approximate expression (15). **Dashed line**: approximate expressions (15a) and (15b). **Dots**: the threshold current obtained from Eq. (13).

The matrix elements $Q_{\nu\nu'}$ define damping and depend on layer sizes weakly. Matrix elements $P_{\nu\nu'} = 0$ for a symmetrical nano-pillar (when the layers have the same

thickness). It means current can excite neither mode in this case.

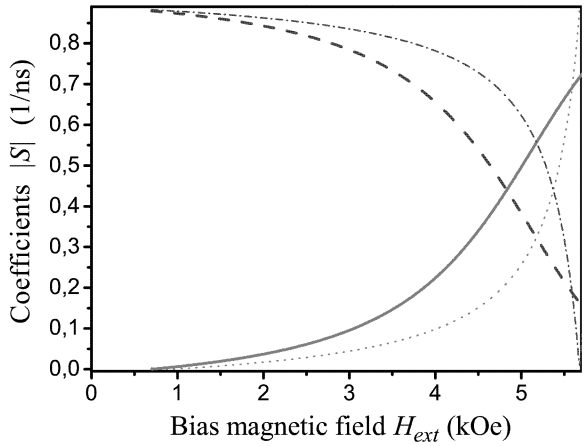

FIG. 8: (color online) The coefficients $|S|$, which show the amplitude of excitation of coupled spin wave modes by microwave magnetic field, as a function of a bias magnetic field. While calculating we put: $L_1/R = 1/10, d/R = 1/25$ and $\mathbf{h}_\sim = \{0, 0.1kOe, 0\}$. **Solid and dashed lines**: The coefficients $|S|$ for lower mode (quasi-antisymmetric one at small bias external fields) and upper mode (quasi-symmetric one at small bias external fields), respectively, obtained from expression (12c) . **Dotted and dashed dotted lines**: The same coefficients $|S|$ obtained from approximate expressions (16a) and (16b).

We can decompose the matrix elements Q_{22} and P_{22} with respect to the ratio L_2/L_1 and restrict ourselves by zero and first nonzero approximations respectively. We have

$$Q_{22} = \gamma(H + 2\pi M(1 - 3\rho_{11} - \rho_{21})), \tag{15a}$$

$$P_{22} = \frac{4\pi M\rho_{21}(-3\rho_{11} + A_3A_2) - H(-3\rho_{11} + A_1A_2)}{2\rho_{21}A_2(4\pi MA_4 - H)} \times \times \sigma_1 \left(1 - \frac{L_2}{L_1}\right), \tag{15b}$$

where A_1, A_2, A_3, and A_4 are dimensionless functions: $A_1 = 3\rho_{11} - \rho_{21}$, $A_2 = C - \ln(L_1/R)$, $A_3 = 2 - 3\rho_{11} - \rho_{21}$, $A_4 = 1 - 3\rho_{11} + \rho_{21}$.

The threshold current for excitation of lower mode, which is quasi-antisymmetric one at small bias fields, as a function of aspect ratio of the second layer L_2/R when external bias magnetic field $H_{ext} = 3kOe$ is represented on Fig. 7.

We will consider the excitation of coupled linear spin wave modes by microwave magnetic field so we consider the Eq. (12) with $I = 0$. The mode for which the absolute value of the coefficient S is larger has larger amplitude and it will be excited by microwave magnetic field.

The coefficients $|S|$ for both modes are represented on Fig. 8. One can see that microwave magnetic field excites upper (quasi-symmetric) mode at small bias fields and lower mode (which passes from quasi-antisymmetric to quasi-symmetric with bias field increase) at large bias fields.

The same way as we get approximate expressions for Q_{22} and P_{22} we can obtain approximate expressions for S_1 and S_2 calculated on the eigenfunctions which correspond to the upper and lower mode respectively. We have

$$S_1 = -\frac{1}{2}h_\sim\gamma + + \frac{3\gamma h_\sim(H - 8\pi M\rho_{21})(\rho_{11} - A_5A_2)}{8\rho_{21}A_2(H - 4\pi MA_4)} \left(1 - \frac{L_2}{L_1}\right), \tag{16a}$$

$$S_2 = -\frac{3\gamma h_\sim(H - 8\pi M\rho_{21})(\rho_{11} - A_5A_2)}{8\rho_{21}A_2(H - 4\pi MA_4)} \left(1 - \frac{L_2}{L_1}\right), \tag{16b}$$

where $A_5 = \rho_{11} - \rho_{21}$. We assumed the vector $\mathbf{h}_\sim$ is directed along y-axis.

VI. CONCLUSIONS

We showed the dipole magnetic field in a two layer nano-pillar can be fully described by two diagonal tensors for every layer: one of them is the usual tensor of demagnetizing coefficients (self-demagnetization tensor), the other one is the cross-demagnetization tensor which describes the dipole-dipole interaction between different layers. Every tensor is fully characterized by only one dimensionless parameter which depends only on relative geometrical sizes of the nano-pillar system.

The spectrum of coupled oscillations of a two-layer nano-pillar consists of two modes with different frequencies. We showed that the lower mode is quasi-antisymmetric at small bias fields and excited by current, the upper mode is quasi-symmetric at small bias fields and excited by microwave magnetic field.

We showed that the frequencies of coupled spin wave modes can be described by the traditional Kittel expression with renormalized bias field and reduced saturation magnetization. The dipole magnetic field leads to effective decrease of magnetization for both modes but this decrease is different for different modes. It does not exceed 10 % for the lower quasi-antisymmetric mode at small bias fields (which is excited by spin-polarized current), and can be 50 % for the upper quasi-symmetric mode at small bias fields (which is excited by microwave magnetic field) For still realistic nano-pillar parameters. But it should be noted these 50 % occur mainly due to the tensor of demagnetizing coefficients (not due to the dynamic dipole-dipole interaction between layers).

[1] A.I. Akhieser, V.G. Baryakhtar, S.V. Peletminsky, *Spin Waves* (Amsterdam, North-Holland, 1967).

[2] L. Berger, Phys. Rev. B **54**, 9353 (1996).

[3] G. Bertotti, I. D. Mayergoyz, and C. Serpico, *Nonlinear Magnetization Dynamics in Nanosystems* (Elsevier Science, Oxford, 2009).

[4] W. Chen, G. de Loubens, J.-M. L. Beaujour, A.D. Kent, and J.Z.Sun, J. Appl. Phys. **103**, 07A502 (2008).

[5] G. Gubbiotti, S. Tacchi, G. Carlotti, T. Ono, Y. Roussigne, V.S. Tiberkevich, and A.N. Slavin, J. Phys.: Condns. Matter **19**, 246221 (2007).

[6] G. Gubbiotti, S. Tacchi, G. Carlotti, P. Vavassori, N. Singh, S. Goolaup, A.O. Adeyeye, A. Stashkevich, and M. Kostylev, Phys. Rev. B **72**, 224413 (2005)

[7] G. Gubbiotti, S. Tacchi, G. Carlotti, N. Singh, S. Goolaup, A.O. Adeyeye, and M. Kostylev, Appl. Phys. Lett. **90**, 092503 (2007)

[8] A.G. Gurevich and G.A. Melkov, Magnetization Oscillations and Waves (CRC Press, New York, 1994)

[9] K.Y. Guslienko, A.N. Slavin, V. Tiberkevich, and S.-K. Kim, Pys. Rev. Lett. **101**, 247203 (2008).

[10] I. Joseph and E. Schlomann, J. Appl. Phys. **36**, 1579 (1965).

[11] S.I. Kiselev, J.C. Sankey, I.N Krivorotov, N.C. Emley, R.J. Schoelkopf, R.A. Buhrman, and D.C. Ralph, Nature **425**, 380 (2003).

[12] S. I. Kiselev, J. C. Sankey, I. N. Krivorotov, N. C. Emley, M. Rinkoski, C. Perez, R. A. Buhrman, and D. C. Ralph, Pys. Rev. Lett. **93**, 036601 (2004).

[13] C. Kittel, *Introduction to Solid State Physics* (Wiley, New York, 1996).

[14] E.M. Lifshits, Zh. Eksp. Teor. Fiz., **15**, 1 (1945).

[15] K. Mizushima, T. Nagasawa, K. Kudo, Y. Saito, and R. Sato, Appl. Phys. Lett. **94**, 152501 (2009).

[16] Y. Nozaki, K. Tateishi, S. Taharazako, S. Yoshimura, and K. Matsuyama, Appl. Phys. Lett. **92**, 161903 (2008).

[17] Y. Nozaki, K. Tateishi, S. Taharazako, S. Yoshimura, and K. Matsuyama, J. Appl. Phys. **105**, 013911 (2009).

[18] R. Sato, Y. Saito, and K. Mizushima, J. Magn. Magn. Mat. **321**, 990 (2009).

[19] J.C. Slonczewski, J. Magn. Magn. Mat. **159**, L1 (1996).

[20] J.C. Slonczewski, J. Magn. Magn. Mat. **195**, L261 (1999).

[21] A. Slavin and V. Tiberkevich, IEEE Trans. Magn. **45**, 1875 (2009).